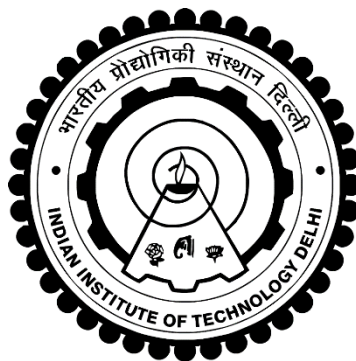


INVESTIGATING DYNAMIC RESPONSE OF THIN SHEET STRUCTURES TOWARDS HIGH RATE OF LOADING

DANISH IQBAL



**DEPARTMENT OF APPLIED MECHANICS
INDIAN INSTITUTE OF TECHNOLOGY DELHI**

JUNE 2019

©Indian Institute of Technology Delhi (IITD), New Delhi, 2019

INVESTIGATING DYNAMIC RESPONSE OF THIN SHEET STRUCTURES TOWARDS HIGH RATE OF LOADING

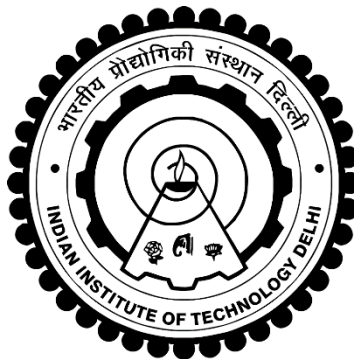
by

DANISH IQBAL

submitted

in fulfilment of the requirements for the degree of Doctor of Philosophy

to the



INDIAN INSTITUTE OF TECHNOLOGY DELHI

JUNE 2019

Dedicated to my Parents & Teachers

CERTIFICATE

The thesis titled “**Investigating Dynamic Response of Thin Sheet Structures towards High Rate of Loading**” being submitted by **Mr. Danish Iqbal** to the Indian Institute of Technology Delhi for the award of the degree of **Doctor of Philosophy**, is a record of original bona-fide research work carried out by him. He has worked under my guidance and supervision and has fulfilled the requirements for the submission of this thesis, which has attained the standard required for a Ph.D. degree of this institute.

The results represented in this thesis have not been submitted elsewhere for the award of any degree or diploma.

Dr. Vikrant Tiwari
Assistant Professor
Department of Applied Mechanics
Indian Institute of Technology Delhi

Place: New Delhi

Acknowledgements

I would like to thank all of my teachers, friends and family members for making this dissertation possible. This work is dedicated to my parents who have immensely inspired me through this long and laborious period. My gratitude can't be expressed in words to my advisor **Dr. Vikrant Tiwari** for his enormous help and guidance throughout my Ph.D. program.

Also, I would also like to thank all my thesis committee members Prof. B.P. Patel, Prof. M.K. Singha and Prof. G.S. Benipal for their invaluable time in reviewing this dissertation and participating in informative discussions. My sincere thanks extends to all the research stuffs and number of students who made this long journey at IITD possible. I would especially like to thank Mehnaz, Amit, Purnashis, Anoop, Kuldeep and Abdul Rehman for their active support during this Ph.D.

Danish Iqbal

Abstract

In this thesis a dedicated research effort has been made to understand the dynamic response of multilayered sheet structures under dynamic and impact loading conditions. Both numerical and experimental evaluations were utilized for the above stated purpose. In chapter 2 and chapter 3 of this thesis a standard SHPB investigation on the dynamic response of the homo-stacked and hetro-stacked configurations was performed. It was established that it is possible to achieve the necessary force equilibrium even for such complex specimens by using pulse shaping technique. A 2 mm thick disc of the specimen material was used as a pulse shaper for homo-stacked specimens. For achieving a force equilibrium in case of hetro-stacked specimens, a composite pulse shaper was employed. Utilizing Johnson-Cook based numerical model and values of inter-layer dynamic coefficients of friction, experimental results were successfully validated. Projectile impact response of monolithic and stacked sheet specimens was evaluated in chapter 4 and chapter 5. A single stage gas gun was instrumental in launching the projectiles while high speed 3D digital image correlation was used in capturing the full-field response of the specimens. The effect of projectile's nose shape and impact velocity on, both, the transient as well as post impact response were investigated in detail. Also, the effect of stacking sequence on the related perforation mechanisms of different projectile shapes was also studied. Closeness of the numerical predictions with experimental outcomes was verified using a suitable error measure criterion.

सार

इस थीसिस में, गतिशील और प्रभाव लोडिंग स्थितियों के तहत बहुस्तरीय शीट संरचनाओं की गतिशील प्रतिक्रिया को समझने के लिए एक समर्पित अनुसंधान प्रयास किया गया है। दोनों संख्यात्मक और प्रायोगिक मूल्यांकन उपर्युक्त उद्देश्य के लिए उपयोग किए गए थे। इस थीसिस के अध्याय 2 और अध्याय 3 में, होमो-स्टैकड और हेट्रो-स्टैकड कॉन्फ़िगरेशन की गतिशील प्रतिक्रिया पर एक मानक SHPB जांच की गई थी। यह स्थापित किया गया था कि पल्स शेपिंग तकनीक का उपयोग करके ऐसे जटिल नमूनों के लिए भी आवश्यक बल संतुलन प्राप्त करना संभव है। 2 मिमी मोटी डिस्क का उपयोग होमो-स्टैकड नमूनों के लिए पल्स शेपर के रूप में किया गया था। हेट्रो-स्टैकड नमूनों के मामले में एक बल संतुलन प्राप्त करने के लिए, एक समग्र पल्स शेपर को नियुक्त किया गया था। जॉनसन-कुक आधारित संख्यात्मक मॉडल का उपयोग और घर्षण के अंतर-परत गतिशील गुणांक के मूल्यों, प्रयोगात्मक परिणामों को सफलतापूर्वक मान्य किया गया। अखंड और स्टैकड शीट नमूनों की प्रोजेक्टाइल प्रभाव प्रतिक्रिया का मूल्यांकन अध्याय 4 और अध्याय 5 में किया गया था। प्रोजेक्टाइल को लॉन्च करने में एक एकल चरण गैस बंदूक का महत्वपूर्ण योगदान था, जबकि नमूनों की पूर्ण क्षेत्रीय प्रतिक्रिया को कैप्चर करने में उच्च गति 3 डी डिजिटल छवि सहसंबंध का उपयोग किया गया था। प्रोजेक्टाइल की नाक के आकार और प्रभाव के वेग पर प्रभाव, दोनों, क्षणिक के साथ-साथ पोस्ट-प्रभाव प्रतिक्रिया की विस्तार से जांच की गई। साथ ही, विभिन्न प्रक्षेप्य आकृतियों के संबंधित छिद्र तंत्र पर स्टैकिंग अनुक्रम के प्रभाव का भी अध्ययन किया गया था। प्रयोगात्मक परिणामों के साथ संख्यात्मक भविष्यवाणियों की निकटता को एक उपयुक्त त्रुटि माप मानदंड का उपयोग करके सत्यापित किया गया था।

Table of Contents

Certificate	iv
Acknowledgements	v
Abstract	vi
List of Figures	ix
List of Tables	xv
1. Relevant Background	1
1.1 Introduction	1
1.2 Motivation for present work	4
1.3 Objective of the present work	5
1.4 Organization of Thesis	6
2. Dynamic Response of Homo-stacked Aluminum and Steel Specimens Subjected to High Strain Rate Loading Conditions	8
2.1 Introduction	8
2.2 Experimental Procedure	11
2.2.1 Split Hopkinson Pressure Bar	11
2.2.2 Specimen Preparation and Nomenclature	14
2.2.3 Pulse Shaping & Dynamic Force Equilibrium	15
2.3 Finite Element Simulations	18
2.4 Results and Discussion	20
2.5 Conclusions	27
3. Dynamic Response of Hetro-stacked Aluminum and Steel Specimens Subjected to High Strain Rate Loading Conditions	28
3.1 Introduction	28
3.2 Experimental Procedure	29
3.2.1 Specimen Preparation and Experiments	31

3.2.2	Pulse Shaping Technique and Force Equilibrium	32
3.2.3	Surface Roughness Measurement	35
3.4	Finite Element Analysis	37
3.5	Results and Discussion	39
3.6	Conclusions	45
4.	Evaluation of monolithic plate response towards different nose shaped projectile impact	46
4.1	Introduction	46
4.2	Experimental Setup	48
4.2.1	Projectiles	50
4.2.2	Target plates and Specimen Preparation	50
4.2.3	Imaging Setup	51
4.3	Numerical Modelling of Impact Experiments	53
4.4	Analysis of Transient Plate Deformation through 3D DIC	56
4.5	Post Impact Macroscopic Analysis	61
4.6	Comparison of Experimental and Simulation Results	62
4.7	Conclusions	68
5.	Evaluation of hetro-stacked target plate response towards different nose shaped projectile impact	70
5.1	Introduction	70
5.2	Experimental Program	73
5.3	Finite Element Simulations	74
5.4	Analysis of Transient Deformation through 3D DIC	75
5.5	Post Impact Analysis	83
5.6	Comparison of Experimental and Numerical Results	85
5.7	Conclusions	92
6.	Conclusions and Future Work	95
6.1	Summary and Conclusions	95
6.2	Recommendations for Future Studies	97
7.	References	98
	List of Publications	109
	Author's Bio-Data	110

List of Figures

Fig. 1.1	Strain rate regimes and associated instrumental techniques.....	1
Fig. 2.1	Schematic of the split Hopkinson pressure bar apparatus used in the present study.....	12
Fig. 2.2	A Typical voltage signal obtained in SHPB experiment.....	13
Fig. 2.3	A typical stress pulse obtained using a pulse shaper showing four stages of pulse shaper deformation.....	15
Fig. 2.4	Comparison of forces at the specimen interfaces, Incident bar end (IB end) and Transmission bar end (TB end) for all four stacking sequences.....	16
Fig. 2.5	(a) Voltage signals obtained without using pulse shaper (b) Forces at specimen ends and force ratio (c) Voltage signals obtained using pulse shaper (d) Forces at specimen ends and force ratio.....	17
Fig.2.6	Incident bar, specimen and transmission bar- experimental setup and FE model.....	19
Fig. 2.7	Comparison of incident, reflected and transmitted strain pulses obtained from experiment and FE simulation.....	20
Fig. 2.8	(a), (b) and (c) True stress versus True strain curves for different stacking sequences for Al-6063-T6 (11R-1-XX) at an approximate strain rates of 500 s^{-1} , 800 s^{-1} and 1000 s^{-1}	21
Fig. 2.9	(a), (b) and (c) True stress versus True strain curves for different stacking sequences for Al-6063-T6 (11R-0.75-XX) at an approximate strain rates of 700 s^{-1} , 900 s^{-1} and 1300 s^{-1}	22

Fig. 2.10	(a) and (b) True stress versus True strain curves for different stacking sequences for Al-6063-T6 (11R-0.5-XX) at an approximate strain rates of 1000 s^{-1} and 1500 s^{-1}	23
Fig. 2.11	(a) and (b) True stress versus True strain curves for different stacking sequences for IS-1570 (mild steel) (MS-11R-0.5-XX) at an approximate strain rates of 500 s^{-1} and 900 s^{-1}	24
Fig. 2.12	(a), (b), (c) and (d) Comparison of experimental and FE simulation curves obtained for Al 6063-T6 (11R-1-XX) at an approximate strain rate of 800 s^{-1}	25
Fig. 2.13	(a), (b), (c) and (d) Comparison of experimental and FE simulation curves obtained for IS-1570 (MS-11R-1-XX) at an approximate strain rate of 500 s^{-1}	26
Fig. 2.14	Evolution of temperature in Al 6063-T6 specimen (11R-1-1/4) at a strain rate of 500 s^{-1}	26
Fig. 3.1	Schematic of the split Hopkinson pressure bar apparatus used in the present study.....	30
Fig. 3.2	A Typical voltage signal obtained in SHPB experiment with pulse shaper.....	30
Fig. 3.3	(a) Voltage signals obtained without pulse shaper (b) Corresponding forces at specimen ends and force ratio (c) Voltage signals obtained with using a composite pulse shaper (d) Corresponding forces at specimen ends and force ratio.....	33
Fig. 3.4	Comparison of forces at the specimen interfaces, Incident bar end (IB end) and Transmission bar end (TB end) for four stacking sequences.....	34

Fig. 3.5	Surface roughness of a typical (a) undeformed and (b, c, d) deformed aluminium specimen at strain rates of 500 s ⁻¹ , 800 s ⁻¹ , 1000 s ⁻¹ respectively.....	35
Fig. 3.6	Schematic representation of increase in surface roughness with increase in applied strain rate.....	37
Fig. 3.7	(a) Meshed model of the hetrostacked specimen, (b) Meshed model of the hetro-stacked specimen between the bars and (c) Comparison of incident, reflected and transmitted strain pulses obtained from experiment and FE simulation.....	38
Fig. 3.8	True stress versus true strain behaviour of family A (a, b, c) and family S (d, e, f) specimens under different strain rates.....	39
Fig. 3.9	(a) and (b) True stress versus strain curves of double layered St-Al and Al-St configurations at three different strain rates of 500, 800 and 1000 s ⁻¹	40
Fig. 3.10	(a-f) Comparison of experimental and FE simulation curves obtained for different stacking configurations at an approximate strain rate of 500 s ⁻¹	42
Fig. 3.11	Evolution of axial strain and von Mises stress in (a, c) Al-St-Al and (b, d) St-Al-St configurations respectively at 500 s ⁻¹	43
Fig. 3.12	Stress-Time history for Al-St-Al and St-Al-St configurations 500 s ⁻¹	44
Fig. 4.1	Schematic of the experimental setup.....	49
Fig. 4.2	(a, b) Projectile dimensions and geometry (c) Target plate dimensions and geometry.....	50

Fig. 4.3	Schematic of stereovision camera measurement system used in the present study.....	52
Fig. 4.4	Mesh density in different regions of the target plate.....	54
Fig. 4.5	Full field out of plane displacement profile of a 0.8 mm thick plate obtained from DIC analysis of (a) blunt and (b) hemispherical projectiles at impact velocities of 131m/s and 128 m/s.....	56
Fig. 4.6	(a-c) Out of plane displacement, (d-f) velocity and (g-i) acceleration for the blunt and hemispherical projectiles on a 0.8 mm thick target plate at the impact velocities of 131 and 128 m/s, respectively.....	58
Fig. 4.7	(a-c) Comparison of out of plane displacements of different target thicknesses for blunt projectile at an impact velocity 204 m/s and (d-e) hemispherical projectile at an impact velocity of 209 m/s.....	59
Fig. 4.8	Maximum out of plane displacement at perforation of point ‘A’ for (a, b) 0.8 mm and (c, d) 1.6 mm thick plate struck by blunt and hemispherical projectile.....	60
Fig. 4.9	Deformed targets of thickness 0.8 mm subjected to (a) blunt nosed projectile at an impact velocity of 131 m/s and (b) hemispherical nosed projectile at an impact velocity of 128 m/s.....	61
Fig. 4.10	Radial cracks around the hole formed due to hemispherical nosed projectile impact in 0.8 mm thick plate at velocities of 128, 204 and 219 m/s.....	62
Fig. 4.11	Time lapse images of the predicted perforation process of (a) blunt projectile with an impact velocity of 131 m/s and (b) hemispherical projectile with an impact velocity of 128 m/s.....	63

Fig. 4.12	Comparison of experimental and numerical full field out of plane displacement contours at various instances.....	64
Fig.4.13	Comparison of experimental and numerical out of plane displacement histories of a 1.6 mm thick plate impacted by blunt (a-c) and hemispherical (d-f) projectiles at velocities of 235 m/s and 251 m/s for points (a, d) 12 mm, (b, e) 18 mm and (c, f) 30 mm from the plate centre.....	65
Fig. 4.14	Comparison of experimental and numerical plug and hole formed in (a) blunt projectile impact at velocity 204 m/s and (b) hemispherical projectile at velocity 219 m/s on 0.8 mm thick plates.....	68
Fig. 5.1	Target dimensions and geometry (dimensions in mm).....	74
Fig. 5.2	Full field out of plane displacement profiles obtained from DIC of (a) blunt and (b) hemispherical projectile impact on St-Al configuration at impact velocities of 219m/s and 225 m/s.....	75
Fig. 5.3	(a-c) Out of plane displacement, (d-f) velocity and (g-i) acceleration for the St-Al configuration impacted by hemispherical and blunt projectiles at an impact velocity of 225 and 219 m/s respectively.....	78
Fig. 5.4	(a-c) Out of plane displacement, (d-f) velocity and (g-i) acceleration for the Al-St configuration impacted by hemispherical and blunt projectiles at an impact velocity of 225 and 219 m/s respectively.....	79
Fig. 5.5	(a-c) Out of plane displacement, (d-f) velocity and (g-i) acceleration for the hemispherical projectile of St-Al and Al-St configurations at an impact velocity of 225 m/s.....	81

Fig. 5.6	(a-c) Out of plane displacement, (d-f) velocity and (g-i) acceleration for the blunt projectile of St-Al and Al-St configurations at an impact velocity of 220 m/s.....	82
Fig. 5.7	Numerically obtained time histories of the transient projectile velocities of (a) hemispherical and (b) blunt projectile.....	83
Fig. 5.8	Actual images of the ejected plugs (Al-St configuration) for blunt and hemispherical projectiles at 220 m/s and 225 m/s impact velocities respectively.....	83
Fig. 5.9	Time lapse images of the predicted perforation process of (a) St-Al and (b) Al-St configurations for hemispherical projectile impact at an impact velocity of 225 m/s.....	86
Fig. 5.10	Comparison of experimental and numerical full field out of plane displacement contours at various instances.....	87
Fig. 5.11	Comparison of experimental and numerical out of plane displacement histories of (a-c) St-Al and (d-e) Al-St configuration impacted by hemispherical projectile at a velocity of 225 m/s for points (a, d) 12 mm, (b, e) 18 mm and (c, f) 30 mm from the plate centre.....	89
Fig. 5.12	Comparison of experimental and numerical out of plane displacement histories of (a-c) St-Al and (d-e) Al-St configuration impacted by blunt projectile at a velocity of 225 m/s for points (a, d) 12 mm, (b, e) 18 mm and (c, f) 30 mm from the plate centre.....	90
Fig. 5.13	Comparison of experimental and numerical plug formed in (a) St-Al, (b) Al-St configuration impacted by hemispherical projectile and (c) St-Al configuration impacted by blunt projectile.....	92

List of Tables

Table 2.1	Chemical composition of Al 6063 T6 and IS 1570.....	14
Table 2.2	Specimen stacking scheme utilized in the study.....	14
Table 2.3	Johnson-Cook parameters for Al 6063-T6 and IS1570.....	18
Table 3.1	Specimen Configuration Scheme utilized in this study.....	32
Table 3.2	Surface Roughness parameters for Al 6063T6.....	36
Table 3.3	Surface Roughness parameters for IS 1570.....	36
Table 3.4	Transient radial elongation in individual specimen layers.....	44
Table 4.1	Chemical Composition of the material under investigation.....	51
Table 4.2	Imaging Setup Parameters.....	53
Table 4.3	Johnson and Cook plasticity and damage parameters for mild steel used in this study.....	55
Table 4.3	Russell Error Criteria.....	66
Table 4.5	Russell Error Measures.....	67
Table 5.1	Details of the double layered impact experiments.....	73
Table 5.2	J-C plasticity and damage parameters for Al 1100-H14 used in this study.....	75
Table 5.3	Experimentally obtained plug and hole dimensions for different configurations.....	84
Table 5.4	Russell Error Measures for Hemispherical Projectile.....	91
Table 5.5	Russell Error Measures for Blunt Projectile.....	91